Space Weather

FEATURE ARTICLE

10.1029/2019SW002187

A Multi-GNSS, Multifrequency, and Near-Real-Time Ionospheric TEC Monitoring System for South America

L. P. O. Mendoza[1,2], **A. M. Meza**[1,2], **and J. M. Aragón Paz**[1,2]

[1]Laboratorio de Meteorología Espacial, Atmósfera Terrestre, Geodesia, Geodinámica, diseño de Instrumental y Astrometría (MAGGIA), Facultad de Ciencias Astronómicas y Geofísicas (FCAG), Universidad Nacional de La Plata (UNLP), La Plata, Argentina, [2]Consejo Nacional de Investigaciones Científicas y Técnicas (CONICET), Buenos Aires, Argentina

Key Points:
- Near-real-time and open-access ionospheric monitoring products are provided
- GPS, GLONASS, Galileo, and BeiDou multifrequency signals are employed
- TEC maps are issued every 15 min with a timeliness of just 3 min

Correspondence to:
L. P. O Mendoza,
lmendoza@fcaglp.unlp.edu.ar

Citation:
Mendoza, L. P. O., Meza, A. M., & Aragón Paz, J. M. (2019). A multi-GNSS, multifrequency, and near-real-time ionospheric TEC monitoring system for South America. *Space Weather*, *17*, 654–661. https://doi.org/10.1029/2019SW002187

Received 21 FEB 2019
Accepted 21 MAR 2019
Accepted article online 8 APR 2019
Published online 3 MAY 2019

Abstract Taking advantage of the public Global Navigational Satellite Systems (GNSS) infrastructure in South America, an operational monitoring system for the total electron content (TEC) in the ionosphere has been developed. It incorporates data in near real time, from more than 90 GNSS satellites tracked by more than 200 ground stations. In turn, the system produces every 15 min a snapshot, that is a map, of the current state of the regional ionosphere, which is immediately available online. These maps could be employed, for example, to augment positioning with single-frequency GNSS receivers. They could also be combined with similar products in order to obtain weighted and reliable regional TEC maps, even in near real time. Most importantly, these products could be employed as data input in space environment forecasting and nowcasting models, given their very short latency of just a few minutes. In order to assess the response of the whole system to severe geomagnetic disturbances, the performance of the whole monitoring system during an actual geomagnetic storm has been investigated. The results suggest that the near-real-time system should be quite capable to monitor the regional TEC at a high temporal rate even under such conditions.

1. Introduction

The total electron content (TEC) is a significant parameter in studying the ionosphere structure and the dynamics of the ionospheric plasma. Then, ionospheric TEC observation and modeling have great importance for many scientific applications and practical services. For instance, global or regional ionospheric TEC mapping can enhance the positioning accuracy of Global Navigation Satellite Systems (GNSS; European GNSS (Galileo) Open Service, 2016; Gao et al., 2006; Le et al., 2009). Also, ionospheric TEC nowcasting and forecasting are employed for monitoring and characterization of geomagnetic storms and ionospheric disturbances generated by space weather activities, such as solar flares, solar energetic particle events, coronal mass ejections, and high-speed solar winds (Meza et al., 2009; Monte-Moreno & Hernández-Pajares, 2014; Van Zele & Meza, 2011; Wang et al., 2016). Moreover, the ionospheric TEC also affects L-band Synthetic Aperture Radar observations (Jehle et al., 2010; Pi, 2015), GNSS reflectometry with space-borne receivers, measurements from altimetry satellite missions (Camps et al., 2016), and also the growing number of microsatellites used in a wide range of applications (Mannucci et al., 2010). In general, the ionospheric TEC plays a key role in the characterization of severe ionospheric disturbances which, in turn, could affect wireless communications, surveying, and navigation, all of them with important social and economic implications (e.g., Fisher et al., 2009; National Research Council, 2009).

Global ionospheric TEC maps (GIMs), derived from GNSS observations, have been developed, analyzed, improved, and routinely produced during the last 20 years (e.g., Hernández-Pajares et al., 1999; Mannucci et al., 1998; Schaer, 1999). In fact, the International GNSS Service (IGS) and its associated Analysis Centers (ACs) have been providing GIMs without interruption, since 1998, with an ever increasing level of reliability, accuracy, and temporal and spatial resolutions (Hernández-Pajares et al., 2009; Schaer & Feltens, 1998). At the same time, due to growing awareness in the public and private sectors on the threats related to space weather, GIMs and also regional GNSS-based TEC maps have become one of the many products employed in forecasting, nowcasting, and characterizing severe events (e.g., Bobrinsky et al., 2011; Moulin et al., 2013; Orús et al., 2007). In Latin America the interest on space weather studies have also increased, particularly

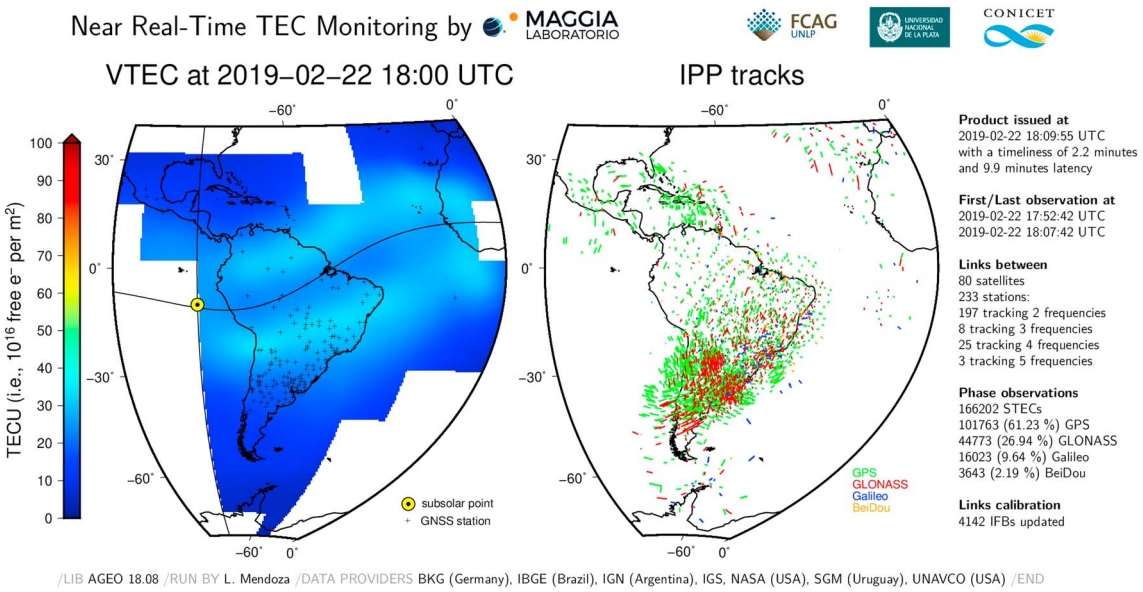

Figure 1. Example of the near-real-time plots produced by the TEC monitoring system, updated every 15 min, and anonymously accessible from wilkilen.fcaglp.unlp.edu.ar/ion/latest.png website. The corresponding TEC maps, in IONEX and NetCDF formats, can be downloaded immediately (wilkilen.fcaglp.unlp.edu.ar/ion/magn/). TEC = total electron content; TECU = TEC unit; IPP = Ionosphere Pierce Point; GLONASS = Global Navigation Satellite System; IFB = Interfrequency Bias; GNSS = Global Navigational Satellite Systems.

in Argentina, Brazil, Mexico, and Peru (Denardini et al., 2016a, 2016b, 2016c; Hysell et al., 2018; Valladares & Chau, 2012). Currently, the Instituto Nacional de Pesquisas Espaciais through the program Estudo e Monitoramento Brasileiro do Clima Espacial (EMBRACE/INPE, Brazil) and the Instituto de Geofísica from the Universidad Nacional Autónoma de Mexico (IGF/UNAM, Mexico), in support to the Laboratorio Nacional de Clima Espacial (LANCE, Mexico), are routinely producing regional GNSS-based TEC maps in order to assimilate them into space weather forecasting models (Gonzalez-Esparza et al., 2016; Takahashi et al., 2016).

Here we present an independent, operational, and GNSS-based ionospheric TEC product. Essentially, a system designed to produce regional TEC maps in almost real time was implemented taking advantage of the significant development of the GNSS infrastructure in South America, including the capability of the installed ground stations to track several GNSS and their modern, multifrequency, signals. Thus, the goal was the incorporation of as many observations as possible, simultaneously keeping the issue delay within the near-real-time standards for GNSS-based products for the atmosphere (i.e., a timeliness of less than 1.5 hr; see, e.g., EUMETNET, 2010). At the same time, the monitoring system was designed to be as independent as possible from external products. In other words, it does not rely on precise satellite orbits, interfrequency biases (i.e., differential code biases), a priori TEC maps, or products of any kind issued by other ACs. Two reasons motivated this strict design specification. First, it helps to enhance the reliability of the monitoring system, as it will not be impacted by unexpected delays or interruptions in the issue of any required product. On the other hand, it simplifies the comparison, or possible combination, of our product with similar ones, given its absolutely independent computation. A comprehensive description of the methods employed, a detailed list of data sources, and results of a preliminary assessment of the system are available in a supplementary technical note (see Mendoza et al., 2019).

2. Product Availability

In general, the near-real-time TEC maps (Figure 1 and Table 1) are available online less than 3 min after the last GNSS observation is acquired (i.e., timeliness of ~3 min), that is, about 10 min after the mean observational epoch of the issued product (i.e., ~10-min latency). These short intervals, achieved thanks to the aggressive parallelization of the analysis system, includes the observational and orbital RINEX (Gurtner & Estey, 2017) files concatenation, the data cleaning (the preprocessing), the Interfrequency Biases calibration, and the vertical TEC representation (the postprocessing, see Mendoza et al., 2019). In practice,

Table 1
Summary of the Characteristics of the Near-Real-Time Ionospheric TEC Monitoring System for South America

Property	Description
Coverage	Central and South America, the Caribbean, Antarctic Peninsula
Modeling	Single-layer vertical TEC model at a height of 450 km
Parametrization	Green's function for a spherical spline (Wessel & Becker, 2008)
Mapping function	Modified single-layer model (Schaer, 1999)
Satellite systems	GPS, GLONASS, Galileo, and BeiDou
Elevation cut off angle	10°
Data rate	15 s
Spatial resolution	0.5 × 0.5°
Sampling rate	15 min
Timeliness	<3 min
Latency	~10 min
Output formats	IONEX and NetCDF
Software	AGEO library (Mendoza et al., 2019) + GMT package (Wessel et al., 2013)

Note. TEC = total electron content; GLONASS = Global Navigation Satellite System.

plots of the current TEC map and the employed satellite-receivers Ionosphere Pierce Point traces, together with a summary of the latest analysis, are updated every 15 min and can be accessed anonymously from wilkilen.fcaglp.unlp.edu.ar/ion/latest.png (or alternatively in Spanish from wilkilen.fcaglp.unlp.edu.ar/ion/ultimo.png). In addition, human readable and binary versions of the maps, in IONEX (Schaer & Feltens, 1998) and NetCDF (Rew & Davis, 1990) formats, can be immediately retrieved (wilkilen.fcaglp.unlp.edu.ar/ion/magn/). In this case, a one-time and simple registration process is required, just writing to the corresponding author briefly stating the intended purpose and requesting for an individual user (and password) to access the TEC product. In turn, registered users would receive, in advance, information of system upgrades or planned operational outages (e.g., due to software or hardware updates).

3. How the St. Patricks's Day Geomagnetic Storm Would Have Been Seen

In order to assess the response of the whole system to severe geomagnetic disturbances, we analyzed GNSS observations acquired during the Saint Patricks's Day geomagnetic storm on 17–18 March 2015 (Astafyeva et al., 2015; Klimenko et al., 2017). Here we employed the very same methodology as for the year-round one-to-one comparisons with IGS products described in Mendoza et al. (2019). However, in this case we produced maps at a higher rate, of 15 min, exactly as the system would have done if it had been running at that time. Then, we compared the resulting maps with global TEC products, provided in IONEX format, and computed by several IGS Ionosphere Associated Analysis Centers: Center for Orbit Determination in Europe (Switzerland; see Schaer, 1999), European Space Agency/European Space Operations Centre (Germany, see Feltens, 2007), IGS (see Hernández-Pajares et al., 2009), Jet Propulsion Laboratory/National Aeronautics and Space Administration (NASA, USA; see Mannucci et al., 1998), and Universitat Politécnica de Catalunya (UPC, Spain; see Hernández-Pajares et al., 1999; Orús et al., 2005). From UPC we employed both their standard and their high rate products. We also included in the analysis TEC products from an additional IGS AC: Wuhan University (China; see Wang et al., 2018). These products are usually available with latencies of a few days or, at best, several hours. In addition, we also included in the intercomparison the (non-IGS) global and high resolution TEC products provided by the Massachusetts Institute of Technology (MIT Haystack Observatory, USA; see Rideout & Coster, 2006).

During this event our maps seem in good agreement with the products from Jet Propulsion Laboratory/NASA and the (combination from the) IGS (Table 2). Also, to lesser extent, with those from UPC and Center for Orbit Determination in Europe. In general, all comparisons result in mean differences and standard deviations larger than the obtained in the year-round analysis (Mendoza et al., 2019). Indeed, the rapid spatial and temporal variability of the physical conditions, naturally associated to a geomagnetic storm, are responsible for the larger discrepancies between the different products and, of course, also between them

Table 2
One-to-One Comparisons Between Selected (GNSS Based) TEC Products, During the St. Patrick's Day Geomagnetic Storm on 17–18 March 2015: codg (CODE), esag (ESA/ESOC), igsg (IGS combination of codg and jplg), jplg (JPL/NASA), mapgps (MIT), upcg (UPC), uqrg (UPC, high rate), whug (WHU), and magn (Our Near-Real-Time Product)

Products				TEC	TEC
A	B	$\bar{x}_{A-B}$	$\bar{\sigma}_{A-B}$	maps	samples
codg	magn	−1.1	5.7	48	22601
	esag	1.9	5.9	24	27048
	igsg	−0.8	1.9	24	27048
	jplg	−1.9	4.6	24	27048
	mapgps	6.0	6.7	48	6840
	upcg	−0.4	4.8	24	27048
	uqrg	−0.5	4.9	48	54096
	whug	1.8	4.5	24	27048
esag	magn	−3.7	8.8	24	11093
	igsg	−2.7	5.8	24	27048
	jplg	−3.8	6.6	24	27048
	mapgps	4.0	7.7	24	3242
	upcg	−2.3	5.0	24	27048
	uqrg	−2.5	7.3	24	27048
	whug	−0.1	4.4	24	27048
igsg	magn	−0.4	5.7	24	11093
	jplg	−1.1	2.6	24	27048
	mapgps	6.8	6.5	24	3242
	upcg	0.4	4.3	24	27048
	uqrg	0.2	4.7	24	27048
	whug	2.6	4.4	24	27048
jplg	magn	0.8	6.2	24	11093
	mapgps	8.1	6.8	24	3242
	upcg	1.4	4.8	24	27048
	uqrg	1.3	5.3	24	27048
	whug	3.7	5.6	24	27048
mapgps	magn	−8.6	7.8	188	425045
	upcg	−5.9	6.9	24	3242
	uqrg	−6.0	6.0	188	25214
	whug	−4.1	7.1	24	3242
upcg	magn	−1.4	7.0	24	11093
	uqrg	−0.2	4.2	24	27048
	whug	2.2	4.7	24	27048
uqrg	magn	−1.1	6.0	192	90231
	whug	2.4	6.2	24	27048
whug	magn	−3.9	7.7	24	11093

Note. The mean difference $\bar{x}_{A-B}$ and mean standard deviation $\bar{\sigma}_{A-B}$, over all compared maps, are expressed in TECU. TEC = total electron content; TECU = TEC unit; GNSS = Global Navigation Satellite Systems; CODE = Center for Orbit Determination in Europe; ESA/ESOC = European Space Agency/European Space Operations Centre; IGS = International GNSS Service; JPL/NASA = Jet Propulsion Laboratory/National Aeronautics and Space Administration; MIT = Massachusetts Institute of Technology; UPC = Universitat Politécnica de Catalunya; WHU = Wuhan University.

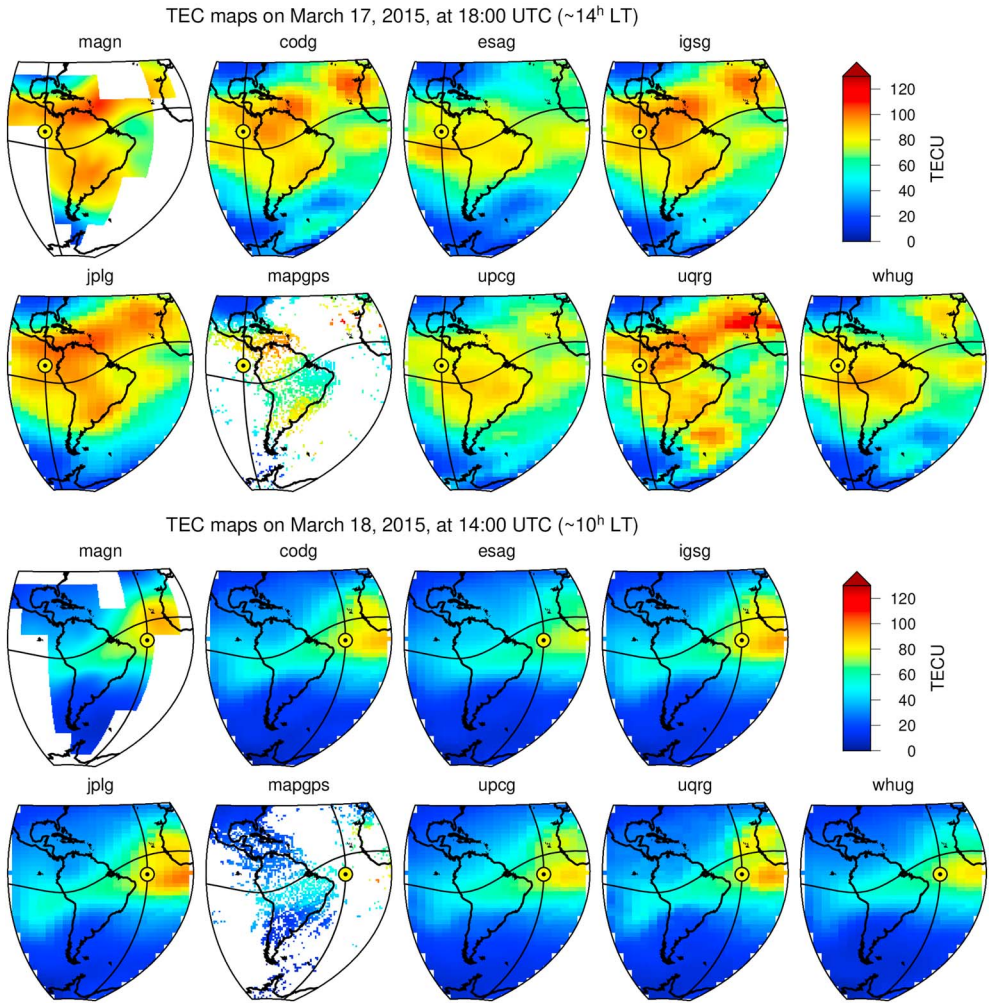

Figure 2. Two snapshots of the regional ionospheric TEC during the St. Patrick's Day geomagnetic storm, on 17–18 March 2015, as seen by codg (Center for Orbit Determination in Europe), esag (European Space Agency/European Space Operations Centre), igsg (International Global Navigational Satellite Systems Service combination of codg and jplg), jplg (Jet Propulsion Laboratory/National Aeronautics and Space Administration), mapgps (Massachusetts Institute of Technology), upcg (UPC), uqrg (UPC, high rate), whug (Wuhan University), and magn (our near-real-time product, provided the system would had been running at that time). For convenience, the subsolar point and the geomagnetic equator are also plotted. TEC = total electron content; TECU = TEC unit; UPC = Universitat Politécnica de Catalunya.

and the actual TEC they are trying to represent. For this reason the map per map comparison reveals significant, spatially localized, differences (Figure 2), with local TEC maxima or minima only *seen* by some of the compared products and not by the others. In these cases, our maps seem to agree more frequently with the high rate maps produced by UPC (i.e., uqrg). This is to be expected, as they are the only compared products that have a sampling rate of 15 min. In other words, the resulting discrepancies are probably due to differences in the mathematical representation (single-layer, multilayer, and tomography), in parametrization (spherical harmonics expansion, spherical spline, bi-cubic splines, and kriging), in the data windowing (5 min, 15 min, 1 hr, and 2 hr), in the number and distribution of ground based GNSS receivers involved and in the combined response of all these different characteristics to the particular physical conditions. In any event, we conclude that our near-real-time monitoring system should be quite capable to monitor the regional TEC, at a high temporal rate and with high spatial resolution, even during periods of severe geomagnetic disturbances. That is, exactly when the products of the system could be most valuable to the research community and other public and private end users.

4. Discussion and Outlook

While the employed observations span all over Central America and the Caribbean, the coverage over South America is not homogeneous. Indeed, the ionosphere over Brazil and southern South America is adequately covered but a large area in the northwest of the subcontinent is, systematically, not optimally observed (Figure 1, right). Although our analysis indicates that the produced maps are also reliable over this area (see Mendoza et al., 2019), the system could clearly benefit in the future from the availability, and subsequent addition, of openly accessible real-time GNSS data streams from stations located in that region. In fact, the system has been designed to be highly scalable, in order to incorporate both additional navigational systems (constellations) and ground stations (networks) without the penalty of a significantly increased latency. Regarding this, it is important to note that our policy, as an independent AC within public research organizations (UNLP and CONICET, Argentina), is to rely exclusively on openly accessible data sources. This has been also the norm within the IGS community since its beginning. This condition ensures the reproducibility of the results and, complemented with the open accessibility of all corresponding derived products, promotes the constructive feedback from other ACs, colleagues, and users. We strictly adhere to this data policy. Then, and in order to better collaborate with the research community, both regional and global, we are willing to incorporate in our system more regional GNSS observations, but we could only consider open-access data providers.

On the other hand, and given the large number of ground stations included in the analysis, and, consequently, the huge number of individual Ionosphere Pierce Points proving the atmosphere (Figure 1, right), the system turns out resilient to the temporal unavailability of observations from particular stations. However, in the uncommon case of unavailability of all streams from a particular data provider (i.e., a caster went off-line), the produced maps could experience a significant degradation in quality and coverage. This is especially problematic in case of data loss from the casters administered by the Instituto Brasileiro de Geografia e Estatística (IBGE, Brazil), by the Instituto Geográfico Nacional (IGN, Argentina), and by UNAVCO (USA), as they provide most of the employed data, with 115, 85, and 41 data streams, respectively. Also, any unreasonable delay in the distribution of the broadcasted orbits and satellite clocks could result in the impossibility to employ any observation from a particular satellite or, even worst, from a particular navigational system. This is due to the limited validity interval of the broadcasted navigational messages. However, during several months of testing the system, we experienced this situation only in very few times.

The system is currently running on a multi-user, nondedicated server, sharing CPU cycles, RAM, and disk storage space with nonrelated processes. In the near future, with proper funding, we expect to correct this nonoptimal operation, gaining in reliability. In addition, the availability of dedicated hardware would allow us to envisage a complementary, a posteriori TEC product, with additional data from those off-line GNSS regional stations, the use of precise satellite orbits and clocks and the implementation of more refined, and time consuming, data cleaning and mapping methodologies. In fact, we expect the presented near-real-time TEC product to evolve over time, as better methodologies are tested and subsequently implemented into the operational monitoring system.

Data Availability Statement

A plot of the most recent TEC map can be accessed anonymously from wilkilen.fcaglp.unlp.edu.ar/ion/latest.png (or alternatively in Spanish from wilkilen.fcaglp.unlp.edu.ar/ion/ultimo.png), whereas registered users can retrieve the TEC maps produced by the system, in IONEX and NetCDF formats, from wilkilen.fcaglp.unlp.edu.ar/ion/magn/ website. A detailed list of all the employed and openly accessible data streams is given in Mendoza et al. (2019). All IGS products were retrieved from ftp://cddis.gsfc.nasa.gov/gnss/products/ionex/ website. The products from MIT were retrieved from http://millstonehill.haystack.mit.edu/ website.

Acknowledgments
We would like to thank the people, organizations, and agencies responsible to collect, compute, maintain, and openly provide the observations, products, and databases that made this work possible. In particular, real-time GNSS orbit and clock messages, along with GNSS observations, are provided by the Bundesamt für Kartographie und Geodäsie (BKG, Germany), in support to the International GNSS Service (IGS), and we particularly thank Peter Neumaier. Real-time GNSS observations are also provided by the Instituto Brasileiro de Geografia e Estatística (IBGE, Brazil), and we particularly thank Sonia Maria Alves Costa; by the Instituto Geográfico Nacional (IGN, Argentina), and we particularly thank Diego Piñón; by the National Aeronautics and Space Administration (NASA, USA), in support to the IGS, and we particularly thank Jennifer Ash from the Crustal Dynamics Data Information System (CDDIS) Team; by the Servicio Geográfico Militar (SGM, Uruguay), and we particularly thank José María also; this material is (partially) based on data services provided by the UNAVCO Facility with support from the National Science Foundation (NSF, USA) and NASA under NSF Cooperative Agreement EAR-0735156 (UNAVCO, USA). The near-real-time TEC monitoring system described in this article is currently running on equipment acquired with funding by the Agencia Nacional de Promoción Científica y Tecnológica (ANPCyT, Argentina), trough the program Fondo para la Investigación Científica y Tecnológica (FONCyT), with grant PICT-2015-1776. Finally, we would like to thank the Editor for the kind support, which made the publication of this article possible. Also, we thank three anonymous reviewers that made constructive comments on the original manuscript.

References

Astafyeva, E., Zakharenkova, I., & Förster, M. (2015). Ionospheric response to the 2015 St. Patrick's Day storm: A global multi-instrumental overview. *Journal of Geophysical Research: Space Physics*, *120*, 9023–9037. https://doi.org/10.1002/2015JA021629

Bobrinsky, N., Moulin, S., Fletcher, E., Luntama, J. P., Pinna, G. M., & Koschny, D. (2011). SSA preparatory programme. *ESA Bulletin*, *147*, 30–41.

Camps, A., Park, H., Foti, G., & Gommenginger, C. (2016). Ionospheric effects in GNSS-Reflectometry from space. *EEE Journal of Selected Topics in Applied Earth Observations and Remote Sensing*, *9*(12), 5851–5861. https://doi.org/10.1109/JSTARS.2016.2612542

Denardini, C. M., Dasso, S., & Gonzalez-Esparza, J. A. (2016a). Review on space weather in Latin America. 1. The beginning from space science research. *Advances in Space Research*, *58*(10), 1916–1939. https://doi.org/https://doi.org/10.1016/j.asr.2016.03.012

Denardini, C. M., Dasso, S., & Gonzalez-Esparza, J. A. (2016b). Review on space weather in Latin America. 2. The research networks ready for space weather. *Advances in Space Research*, *58*(10), 1940–1959. https://doi.org/https://doi.org/10.1016/j.asr.2016.03.013

Denardini, C. M., Dasso, S., & Gonzalez-Esparza, J. A. (2016c). Review on space weather in Latin America. 3. The research networks ready for space weather. *Advances in Space Research*, *58*(10), 1960–1967. https://doi.org/https://doi.org/10.1016/j.asr.2016.03.011

EUMETNET (2010). EIG EUMETNET GNSS water vapour programme (E-GVAP-II). techreport, Version 1.0, Avenue Circulaire 3, 1180 Bruxelles, Belgique European Meteorological Services Network. Retrieved from http://egvap.dmi.dk/support/formats/egvap_prd_v10.pdf

European GNSS (Galileo) Open Service (2016). Ionospheric correction algorithm for Galileo single frequency users. techreport 1.2, European Commission. Retrieved from https://www.gsc-europa.eu/system/files/galileo_documents/Galileo_Ionospheric_Model.pdf

Feltens, J. (2007). Development of a new three-dimensional mathematical ionosphere model at European Space Agency/European Space Operations Centre. *Space Weather*, *5*, S12002. https://doi.org/10.1029/2006SW000294

Fisher, G., Meehan, J., & Murtagh, W. (2009). Understanding space weather customers in GPS-reliant industries. *Space Weather*, *8*, 06003. https://doi.org/10.1029/2009SW000556

Gao, Y., Zhang, Y., & Chen, K. (2006). Development of a real-time single-frequency precise point positioning system and test results. In *Proceedings of the 19th International Technical Meeting of the Satellite Division of The Institute of Navigation (ION GNSS 2006)* (pp. 2297–2303). Fort Worth, TX.

Gonzalez-Esparza, J. A., De la Luz, V., Corona-Romero, P., Mejia-Ambriz, J. C., Gonzalez, L. X., Sergeeva, M. A., & Aguilar-Rodriguez, E. (2016). Mexican Space Weather Service (SCiESMEX). *Space Weather*, *15*, 3–11. https://doi.org/10.1002/2016SW001496

Gurtner, W., & Estey, L. (2017). RINEX: The receiver independent exchange format version 3.03, Update 1. techreport, International GNSS Service (IGS). Retrieved from ftp://igs.org/pub/data/format/rinex303.pdf

Hernández-Pajares, M., Juan, J., & Sanz, J. (1999). New approaches in global ionospheric determination using ground GPS data. *Journal of Atmospheric and Solar-Terrestrial Physics*, *61*(16), 1237–1247. https://doi.org/https://doi.org/10.1016/S1364-6826(99)00054-1

Hernández-Pajares, M., Juan, J. M., Sanz, J., Orus, R., Garcia-Rigo, A., Feltens, J., & Krankowski, A. (2009). The IGS VTEC maps: A reliable source of ionospheric information since 1998. *Journal of Geodesy*, *83*(3), 263–275. https://doi.org/10.1007/s00190-008-0266-1

Hysell, D. L., Baumgarten, Y., Milla, M. A., Valdez, A., & Kuyeng, K. (2018). Ionospheric specification and space weather forecasting with an HF beacon network in the Peruvian sector. *Journal of Geophysical Research: Space Physics*, *123*, 6851–6864. https://doi.org/10.1029/2018JA025648

Jehle, M., Frey, O., Small, D., & Meier, E. (2010). Measurement of ionospheric TEC in spaceborne SAR data. *IEEE Trans. Geosci. Remote Sens.*, *48*(6), 2460–2468. https://doi.org/10.1109/tgrs.2010.2040621

Klimenko, M., Klimenko, V., Despirak, I., Zakharenkova, I., Kozelov, B., Cherniakov, S., & Ratovsky, K. (2017). Disturbances of the thermosphere-ionosphere-plasmasphere system and auroral electrojet at 30° E longitude during the St. Patrick's Day geomagnetic storm on 17–23 March 2015. *Journal of Atmospheric and Solar-Terrestrial Physics*, *180*, 78–92. https://doi.org/10.1016/j.jastp.2017.12.017

Le, A., Tiberius, C., van der Marel, H., & Jakowski, N. (2009). Use of global and regional ionosphere maps for single-frequency precise point positioning. In M. G. Sideris (Ed.), *Observing our changing Earth* (Vol. 133, pp. 759–769). Berlin, Heidelberg: Springer. International Association of Geodesy Symposia. https://doi.org/https://doi.org/10.1007/978-3-540-85426-587

Mannucci, A. J., Dickson, J., Duncan, C., & Hurst, K. (2010). GNSS Geospace Constellation (GGC): A CubeSat space weather mission concept. techreport, Washington, DC 20001, National Academy of Sciences, http://www8.nationalacademies.org/SSBSurvey/DetailFileDisplay.aspx?id=881, Committee on a Decadal Strategy for Solar and Space Physics (Heliophysics), Request for Information Response Number 176.

Mannucci, A. J., Wilson, B. D., Yuan, D. N., Ho, C. H., Lindqwister, U. J., & Runge, T. F. (1998). A global mapping technique for GPS-derived ionospheric total electron content measurements. *Radio Science*, *33*(3), 565–582. https://doi.org/10.1029/97RS02707

Mendoza, L. P. O., Meza, A. M., & Aragõn Paz, J. M. (2019). Technical note on the multi-GNSS, multi-frequency and near real-time ionospheric TEC monitoring system for South America. *EarthArXiv*. https://doi.org/10.31223/osf.io/3vts6

Meza, A., Van Zele, M. A., & Rovira, M. (2009). Solar flare effect on the geomagnetic field and ionosphere. *Journal of Atmospheric and Solar-Terrestrial Physics*, *71*(12), 1322–1332. https://doi.org/10.1016/j.jastp.2009.05.015

Monte-Moreno, E., & Hernández-Pajares, M. (2014). Occurrence of solar flares viewed with GPS: Statistics and fractal nature. *Journal of Geophysical Research: Space Physics*, *119*, 9216–9227. https://doi.org/10.1002/2014JA020206

Moulin, S., Luntama, J. P., & Bobrinsky, N. (2013). Space situational awareness—Space weather PSD. techreport, European Space Agency, http://swe.ssa.esa.int/DOCS/SSA-SWE/SSA-SWE-RS-SSD-0001_i1r3.pdf, Issue 1, Rev. 3, ESA SSA Team. ,

National Research Council (2009). *Severe space weather events—Understanding societal and economic impacts: A workshop report: Extended summary*. Washington, DC: National Academies Press. https://doi.org/10.17226/12643

Orús, R., Cander, L. R., & Hernández-Pajares, M. (2007). Testing regional vertical total electron content maps over Europe during the 17–21 January 2005 sudden space weather event. *Radio Science*, *42*, RS3004. https://doi.org/10.1029/2006RS003515

Orús, R., Hernández-Pajares, M., Juan, J., & Sanz, J. (2005). Improvement of global ionospheric VTEC maps by using kriging interpolation technique. *Journal of Atmospheric and Solar-Terrestrial Physics*, *67*(16), 1598–1609. https://doi.org/10.1016/j.jastp.2005.07.017

Pi, X. (2015). Ionospheric effects on spaceborne synthetic aperture radar and a new capability of imaging the ionosphere from space. *Space Weather*, *13*, 737–741. https://doi.org/10.1002/2015SW001281

Rew, R., & Davis, G. (1990). NetCDF: An interface for scientific data access. *IEEE Computer Graphics and Applications*, *10*(4), 76–82. https://doi.org/10.1109/38.56302

Rideout, W., & Coster, A. (2006). Automated GPS processing for global total electron content data. *GPS Solutions*, *10*, 219–228. https://doi.org/10.1007/s10291-006-0029-5

Schaer, S. (1999). Mapping and predicting the Earth's ionosphere using the Global Positioning System (Phd thesis), Universität Bern, Philosophisch-naturwissenschaftlichen Fakultät.

Schaer, S., & Feltens, J. (1998). IONEX: The IONosphere Map EXchange Format version 1. techreport, Astronomical Institute, University of Berne, Switzerland and ESA/ESOC, Darmstadt, Germany. Retrieved from http://ftp.aiub.unibe.ch/ionex/draft/ionex11.pdf, September 17, 2015, update to v1.1.

Takahashi, H., Wrasse, C. M., Denardini, C. M., Pádua, M. B., de Paula, E. R., Costa, S. M. A., & Sant'Anna, N. (2016). Ionospheric TEC weather map over South America. *Space Weather*, *14*, 937–949. https://doi.org/10.1002/2016sw001474

Valladares, C. E., & Chau, J. L. (2012). The low-latitude ionosphere sensor network: Initial results. *Radio Science*, *47*, RS0L17. https://doi.org/10.1029/2011RS004978

Van Zele, M. A., & Meza, A. (2011). The geomagnetic solar flare effect identified by SIIG as an indicator of a solar flare observed by GOES satellites. *Advances in Space Research*, *48*, 826–836. https://doi.org/10.1016/j.asr.2011.04.037

Wang, C., Rosen, I. G., Tsurutani, B. T., Verkhoglyadove, O. P., Meng, X., & Mannucci, A. J. (2016). Statistical characterization of ionosphere anomalies and their relationship to space weather events. *Journal of Space Weather and Space Climate*, *6*, A5. https://doi.org/10.1051/swsc/2015046

Wang, C., Shi, C., Fan, L., & Zhang, H. (2018). Improved modeling of global ionospheric total electron content using prior information. *Remote Sensing*, *10*(1), 63. https://doi.org/10.3390/rs10010063

Wessel, P., & Becker, J. M. (2008). Interpolation using a generalized Green's function for a spherical surface spline in tension. *Geophysical Journal International*, *174*(1), 21–28. https://doi.org/10.1111/j.1365-246x.2008.03829.x